Environ. Sci. Technol. **2008,** *42,* 3556–3562

Coupled Effect of Chemotaxis and Growth on Microbial Distributions in Organic-Amended Aquifer Sediments: Observations from Laboratory and Field Studies

MENG WANG,[†] ROSEANNE M. FORD,*[,†] AND RONALD W. HARVEY[‡]

Department of Chemical Engineering, University of Virginia, Charlottesville, Virginia 22904, and United States Geological Survey, Boulder, Colorado 80303

Received September 23, 2007. Revised manuscript received February 23, 2008. Accepted February 29, 2008.

The inter-relationship of growth and chemotactic response exhibited by two common soil-inhabiting bacteria was investigated to determine its impact on bacterial migration. Filter-chambers were used to simulate aquifer sediments characterized by vertical gradients of organic contaminants in both artificial groundwater flow systems in the laboratory and within the screened intervals of observation wells in a sandy aquifer. A labile model contaminant (acetate) was added to the top compartments of the three-part chambers, whereas bacteria with a demonstrated propensity to grow on and chemotactically respond to acetate were introduced to the lower compartments. The motility and chemotactic response of *Pseudomonas putida* F1 resulted in 40 to 110% greater abundances in the upper compartments and concomitant 22 to 70% depletions in the lower compartments relative to the nonchemotactic controls over 2 days. Bacteria were in greatest abundance within the sand plug that separated the upper and lower compartments where sharp acetate gradients induced a strong chemotactic response. This observation was consistent with predictions from a mathematical model. In agreement with the laboratory results, the down-well filter-chamber incubations with *Pseudomonas stutzeri* in the aquifer indicated that 91% fewer bacteria resided in the lower compartment than the control experiment without acetate at 15 h. The combination of chemotaxis and growth greatly accelerated the migration of bacteria toward and subsequent abundance at the higher acetate concentration.

Introduction

Restoration of aquifers contaminated by recalcitrant organic compounds has proven to be a difficult task (*1, 2*). Because of the properties of low solubility, low volatility, low intrinsic reactivity, and low release rates from soil or sediments, those contaminants, such as petroleum, crude oil, coal tars, and chlorinated hydrocarbons, persist in groundwater for several years and leave behind a residue even after treatment by physicochemical cleanup schemes. Bioremediation, which provides a safer, more efficient and less expensive approach, is an effective alternative solution to eliminate the contaminants. However, this process is often hindered by transport limitations of the degrading bacterial populations that are preferentially transported through zones characterized by high permeability (*3, 4*). Chemotaxis, the ability of bacteria to sense chemical concentration gradients and to migrate preferentially toward locations favorable to their survival, is expected to enhance bioremediation in zones of low permeability by directing bacteria toward contaminants that are concentrated in such zones (*5–8*).

Many subsurface bacteria exhibit chemotactic responses toward the recalcitrant contaminants that they degrade (*9, 10*) because the contaminants can serve as carbon and energy sources for growth (*11, 12*). The soil-inhabiting strain, *Pseudomonas putida*, was chemotactic to chlorinated hydrocarbons that were perceived as potential substrates (*13, 14*). Microbial population migration in response to chemoattractants also has been reported. Witt et al. (*15*) noted an unexpectedly high bacterial migration velocity of *Pseudomonas stutzeri* KC in carbon tetrachloride-contaminated sand columns and attributed it to the chemotactic influences from nitrate gradients induced by the depletion of nitrate during carbon tetrachloride degradation.

Chemotaxis in aqueous systems has been well-demonstrated and characterized in laboratory studies (*7, 16–19*). However, chemotaxis in porous media only recently was identified and documented (*20–23*). Pedit and co-workers (*22*) used a capillary filled with glass beads to simulate the porous media and indicated that the accumulation of *P. putida* G7 was higher in the capillaries initially containing naphthalene than in the controls. A statistically significant chemotactic response in porous media was reported by Olson et al. (*21*). They observed a strong chemotactic accumulation of *P. putida* F1 toward trichloroethylene in a glass-coated polystyrene bead-packed column by the adoption of Sherwood et al.'s (*24*) magnetic resonance imaging method. Roush et al. (*23*) also suggested that chemotaxis could be enhanced in a heterogeneous medium by examining swarm plates with a rectangular-shaped sand-filled area.

Most of the chemotaxis studies were conducted over short time periods, ranging from several minutes to a few hours, with conservative attractants selected to reduce complexity in the analysis of chemotaxis. Consequently, the growth of bacteria was minimal and usually neglected. However, bioremediation operations occur over much longer time scales, and the biomass growth upon the attractant was considered to be critical to enhance biodegradation. Although the positive feedback between contaminant consumption, microbial growth, and chemotaxis in bioremediation processes has been noted, the descriptions have been qualitative without substantial experimental or mathematical analysis (*25–27*).

Thus, the objective of this study was to investigate the effects of chemotaxis on bacterial migration over longer time periods than most previously reported laboratory studies, specifically for durations long enough to allow significant biomass growth on a consumable attractant. To represent an aquifer in which contaminants may be sequestered in zones of lower hydraulic conductivity that are spatially separated from more conductive zones involved in bacterial transport, compartmentalized filter-chambers with different conductive zones were employed. Each filter-chamber housed two compartments separated by a sand plug: the attractant compartment represented a contaminant reservoir, the bacteria compartment characterized a highly permeable

* Corresponding author phone: (434)924-6283; fax: (434)982-2658; e-mail: rmf3f@virginia.edu.
[†] University of Virginia.
[‡] United States Geological Survey.

10.1021/es702392h CCC: $40.75

Published on Web 04/15/2008

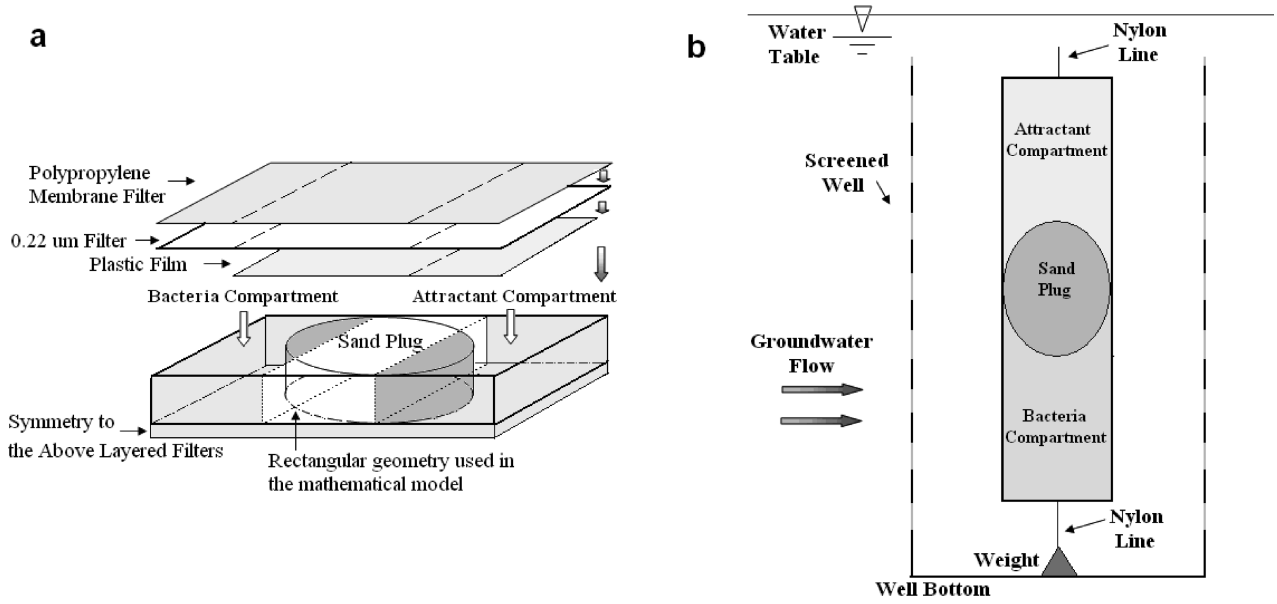

FIGURE 1. (a) Structure of the filter-chamber. A sand plug that was encircled by a polypropylene membrane separated the bacteria and attractant compartments. The rectangular geometry of the sand plug used in the mathematical model is superposed. An outer polypropylene membrane filter provided structural support, a 0.22 μm mixed cellulose ester filter prevented bacteria from leaving the chamber, and a plastic film that covered only the attractant compartment and the sand plug prevented loss of the attractant from those locations. (b) Orientation of the filter-chamber in the well in the field study. The orientation of the filter-chamber in the laboratory experiments was the same but within an AGW system.

layer, and the sand plug mimicked the aquifer sediments between the two. Compartments were sampled, and bacterial counts were compared to two different controls. Differences in intercompartment bacterial distributions between the chemotactic experiments and the controls were assessed using a mathematical model to elucidate the contributions of chemotaxis and growth. The filter-chambers also were deployed at the field site in Cape Cod, MA to determine as to whether similar distribution trends occurred under conditions that were closer to those of a natural groundwater environment.

Experimental Procedures

Bacterial Strains and Buffered Solutions in Laboratory Studies. All laboratory experiments were performed using *P. putida* F1, which was provided by Caroline Harwood (*10*). Artificial groundwater (AGW), prepared to match the major ion concentrations reported for previous studies at the Cape Cod, MA field site, was used as the buffer solution for this study (*28, 29*). Bacteria grown in pH-adjusted (pH 4.5–5.6) AGW augmented with 20 mM acetate and 30 mM urea were harvested at an optical density (OD) value of 0.6 (Beckman, DU-7) after approximately 36 h in a Lab-line Enviro-shaker (Model 3528-5) at 150 rpm, 27 °C and were suspended in 10% random motility buffer (*30*). Nonchemotactic bacterial controls were obtained by mechanically shearing off the flagella from bacteria by passing the bacterial suspension vigorously through a 2.5 cm, 26-gauge stainless steel needle (Becton-Dickinson) (*31*). Without flagella, the bacteria were not able to swim and therefore were incapable of exhibiting a chemotactic response to the attractant. Bacteria without flagella were observed to grow at the same rate as those with flagella. Because the same strain of bacteria was used for both test and nonchemotactic control systems, their other properties, except for motility and chemotaxis behaviors, were assumed to be the same.

Filter-Chamber Structure. The filter-chamber was constructed as indicated in Figure 1a. A sand plug encircled by polypropylene membrane mesh (210 mesh, 34% open area, 308 μm thickness) divided the chamber into three sections: the bacteria compartment, the sand plug, and the attractant compartment. Sand collected from the site of our field study was sieved to obtain a sediment fraction with grain diameters ranging from 0.42 to 0.85 mm (*32*). Sieved sand was treated by washing with 0.5 M HCl and deionized water to remove a fraction of the grain-surface mineral coatings to minimize bacterial immobilization (*33, 34*).

An impermeable plastic film was layered over the sand plug and the attractant compartment to prevent the loss of attractant to the surroundings in the upper portion of the chamber (Figure 1b). In contrast, the bacteria compartment in the lower portion was not sealed by this water-impermeable layer. The faces along the entire length of the filter-chamber were covered by a filter of mixed cellulose esters (0.22 μm pore diameter, Millipore, GSWP14250). This filter retained bacteria within the entire chamber but allowed exchange of dissolved constituents between the bacteria compartment and the surrounding environment. An outer layer of polypropylene mesh was used to provide structural rigidity to support the inner membranes and to protect the filters from damage by abrasion.

The chamber was initially filled with AGW augmented with 30 mM urea. The addition of urea provided an abundant nitrogen source such that acetate became the growth-limiting substrate (*35*). The bacterial abundance in the injection solution was kept constant for each trial. Then, 100 μL of bacterial suspension ($\sim 10^9$ cells/mL) and 150 μL of 1 M acetate were introduced into opposite ends of the filter-chambers to reach final concentrations of $\sim 5 \times 10^6$ cells/mL in the bacteria compartment and 20 mM in the attractant compartment. Syringes were inserted into opposite ends of the chamber to extract samples from both compartments simultaneously, and bacteria were enumerated by the Acridine Orange counting method (*36*). A chamber was sacrificed after it was sampled.

The whole chamber was placed into a 5 L bucket, where 4.5 L of AGW with 30 mM urea was stirred to simulate groundwater flow. The filter-chamber was oriented perpendicular to the AGW flow direction, with the attractant compartment above the bacteria compartment. In this

orientation, the migration of bacteria to the upper sections was solely attributable to bacterial motility and chemotaxis. Because the bacteria compartment was not covered by the water-impermeable film, solutes and dissolved gases were able to move through the membrane barrier filters. Under this condition, nitrogen and oxygen were provided continuously to the bacteria through the lower compartment, and the effects due to other nutrient limitations were decreased.

Field Site Filter-Chamber Studies. Filter-chambers were suspended individually in separate wells (F513-A through F513-F), spaced ~1 m apart along a line perpendicular to groundwater flow and screened at the same depth. The wells are located in a gravel pit immediately south of the Massachusetts Military Reservation in Cape Cod, MA (*29, 37, 38*). Three filter-chambers received an amendment of 0.1 mM acetate, whereas the three others serving as controls did not. The initial bacterial abundance was the same in all six filter-chambers. Groundwater bacteria *P. stutzeri* isolated from an aquifer in New Hampshire (*39*) were selected as the test organisms in these in situ studies. Sand collected from the gravel pit was used directly to create the sand plugs without any treatments. Weights were attached to the bottoms of the chambers, which were then lowered down the wells using monofilament nylon line and suspended within the screened intervals at the bottoms of the wells (Figure 1b). After 15 h, the chambers were removed from the wells. Samples were drawn from each compartment. The bacteria were stained with DAPI (4′,6-diamidino-2-phenylindole, Sigma Chemical Co., No. D1388) and subsequently enumerated using epifluorescence microscopy (*40*).

Mathematical Model. A conservation equation was applied to describe the bacterial transport and growth in porous media under the influence of acetate as follows (*41, 42*):

$$\theta\frac{\partial c}{\partial t}+\frac{\partial s}{\partial t}=\left(\frac{\theta}{\tau}D_{cx}\right)\frac{\partial^2 c}{\partial x^2}-\frac{\partial(\theta c V_{cx})}{\partial x}+\left(\frac{\mu_m a}{K_s+a}\right)c \qquad (1)$$

with terms for sorption, diffusion, chemotaxis, and growth, in which c and s are bulk and surface attached bacterial abundances, respectively, θ is the porosity, τ is the tortuosity, x is the transport distance in the direction of the gradient, t is elapsed time, and D_{cx} is the bacterial random motility coefficient. The bacterial abundance on the solid phase was calculated according to $s = K\theta c$, in which K is an equilibrium constant for adsorption and desorption. Chemotaxis is described as an advection term based on empirical observations (*43*) and is dependent on both attractant concentration and gradient. Under the condition of a shallow attractant gradient, as in the filter-chamber, the chemotactic velocity, V_{cx}, is described by

$$V_{cx}=\frac{1}{3}\left(\chi_o\frac{K_c}{(K_c+a)^2}\frac{\partial a}{\partial x}\right) \qquad (2)$$

where χ_o is the chemotactic sensitivity coefficient, K_c is the chemotactic binding constant, and a is the attractant concentration (*44*). Acetate was verified as the growth-limiting nutrient at the concentration used in the experiment. Therefore, the growth term in eq 1 was represented by the Monod model (*45*). Correspondingly, the conservation equation for the attractant, which was coupled with bacterial abundance, had the form

$$\frac{\partial a}{\partial t}=D_{ax}\frac{\partial^2 a}{\partial x^2}-\frac{\mu_m a}{(K_s+a)Y_{x/s}}c \qquad (3)$$

with the attractant consumption term proportional to the bacterial abundance, where D_{ax} is the attractant diffusion coefficient, μ_m is the theoretical maximum growth rate, K_s is the half-saturation constant for the growth, and $Y_{x/s}$ is the yield coefficient with respect to carbon. Eqs 1−3 were applied to the sand plug. Because the bacteria compartment allowed the exchange of small water-soluble molecules with the surroundings providing a supply of oxygen and a loss of attractant, the attractant conservation equation was modified by the addition of a loss term written as

$$\frac{\partial a}{\partial t}=D_{ax}\frac{\partial^2 a}{\partial x^2}-\frac{\mu_m a}{(K_s+a)Y_{x/s}}c-k_m a \qquad (4)$$

where k_m is the mass transfer coefficient for the attractant between the bacteria compartment and the surrounding AGW. For the interfaces between each compartment, equal-flux conditions were applied for both bacteria and attractant transport, whereas for the boundaries of the filter-chamber, no-flux conditions were used.

This mathematical model was solved numerically by a finite-difference method using a MATLAB code and was fitted to the data in each compartment simultaneously. We used literature values for porous media characteristics and fundamental bacterial properties, including $D_{ax} = 1.19 \times 10^{-5}$ cm^2/s at 25 °C (*45*), $\chi_o = 2.3 \times 10^{-4}$ cm^2/s (*20*), $K_s = 2.14 \times 10^{-5}$ M (*46*), $Y_{x/s} = 1.045 \times 10^{14}$ cell/M (*46*), $K = 0.32$, $\theta = 0.37$, and $\tau = 1$ (*47*). Because bacterial growth under the specific filter-chamber conditions could not be measured independently, we used the literature values for K_s and $Y_{x/s}$ but fitted the most sensitive growth parameter μ_m. We fitted μ_m (0.11 h^{-1}), D_{ax} (7.5×10^{-6} cm^2/s), and k_m (0.003 h^{-1}) to match the specific nutrient conditions and mass transport resistance in the filter-chamber in the laboratory systems. The chemotactic binding constant K_s (8.5×10^{-4} M) used in the model was fitted within a range of values reported in the literature (*19*).

Results and Discussion

Chemotactic *P. putida* F1 and Control without Acetate. Bacterial abundances in both lower and upper compartments were sampled at several time points in controlled laboratory experiments using an initial acetate concentration of 20 mM. Results are plotted in Figure 2a,b. Substantial bacterial growth was observed in the presence of acetate. As indicated in Figure 2b, the bacterial abundance in the bacteria compartment, after an initial decrease from their starting value of 5×10^6 cells/mL, reached 10^7 cells/mL after 24 h and increased ~10-fold over the initial abundance after 70 h. In contrast, for the attractant compartment (Figure 2a), the bacterial abundance showed an upward trend over the first 48 h and reached a maximum population of 3.5×10^7 cells/mL. However, at 78 h, the bacterial abundance in the attractant compartment began to decrease, presumably because of a buildup of toxic metabolic products. In contrast, there was no decrease in the bacterial abundance in the bacteria compartment, which was exposed to oxygenated AGW. As compared to the experiments with acetate, the control without acetate had comparably low populations in both compartments that decreased in magnitude over time because of bacterial death. Greater bacterial accumulation in the attractant compartment as compared to the control without acetate was consistent with our expectation for a combination of chemotaxis toward and growth on acetate. In contrast, the bacterial distribution in chambers without acetate was controlled mainly by bacterial motility, which allowed the bacterial population to migrate to the attractant compartment. However, no growth occurred in the attractant compartment because of carbon limitation. Starvation conditions in the control chambers were consistent with our observations of an apparent decrease in cell size over time.

In the presence of acetate, the bacterial abundance at 13 h in the bacteria compartment (Figure 2b) was lower than the initial concentration and the control. The greater initial decrease with acetate as compared to the control was

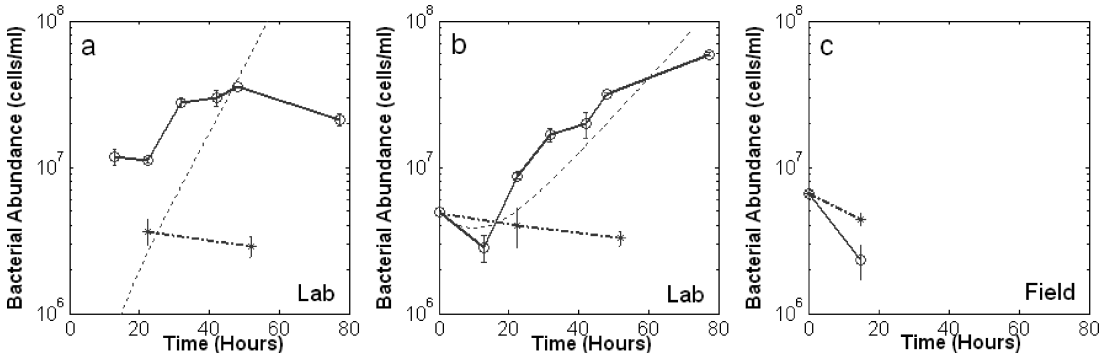

FIGURE 2. Changes in bacterial abundances over time in (a) the attractant compartment, (b) the bacteria compartment of the laboratory experiments, and (c) the bacteria compartment of the field study. Symbols represent the following: -○-, experimental data for chemotactic bacteria with acetate; ----, simulation results for chemotactic bacteria with acetate; and -*-, experimental data for the control experiment without acetate. In panels a and b, the standard deviation was calculated from counting processes except for the value at 48 h, which was the standard deviation from three replicates of the same experimental trial. The initial bacterial abundance estimated as 5×10^6 cells/mL was based on the known bacterial abundance in the injectate. The initial bacterial abundance in the attractant compartment (estimated to be less than 10^5 cells/mL) is not plotted because of the semilogarithmic coordinate. In panel c, the bacterial abundance in the bacteria compartment with acetate (three replicates for each) was statistically lower than the no-acetate control ($p = 0.05$). The groundwater at the site had an indigenous organism population of $(2.22 \pm 0.4) \times 10^5$ cells/mL, which was neglected.

attributed to the chemotactic migration away from the bacteria compartment and toward the source of acetate. The mass exchange of small molecules in the lower compartment with the surrounding AGW was assumed to maintain a constant low acetate concentration within the bacteria compartment. Consequently, a sharp acetate gradient across the sand plug was continuously maintained and stimulated the migration of bacteria from the lower compartment to the higher one. At subsequent times, the bacterial abundance in the presence of acetate exceeded the control case due largely to bacterial growth on acetate. Although chemotaxis was still expected to occur, it was difficult to detect in the presence of substantial microbial growth. The effect of chemotaxis was apparent at early times as more bacteria migrated out of the bacteria compartment under the influence of the chemoattractant. At later times, growth dominated.

Because the two compartments and the interstitial spaces of the sand plugs within the filter-chambers contained limited volumes of water, only the averaged bacterial abundances were able to be measured from each compartment. Consequently, detailed information on the bacterial abundance along the length of the filter-chamber was not available. Therefore, a mathematical model was developed to elucidate the coupled impact on the bacteria by chemotaxis and growth.

The mathematical model accurately predicted the chemotaxis-induced depletion in abundance within the bacteria compartment (Figure 2b) but overestimated the growth rate in the attractant compartment (Figure 2a) at later times. The simulation closely approximated the chemotactic response in the bacteria compartment, which was predicted by the experimental data. The simulated bacterial accumulation in the attractant compartment was extremely sensitive to the change of bacterial abundance at the initial stage because of the large amount of acetate present. With the assumption of a rectangular-shaped sand plug (Figure 1a), the one-dimensional mathematical model underestimated the response from the initial migration of bacteria into the attractant compartment across the short length of the elliptical sand plug. Although the elliptical shape of the sand plug was not optimal for modeling the system, our simple one-dimensional model focusing on the key processes was nevertheless useful in analyzing and understanding the relative contributions of chemotaxis and growth to observe bacterial transport and distribution within the filter-chambers.

Chemotactic *P. putida* F1 and Nonchemotactic Control. It was observed that chemotactic bacteria were 22–70% less abundant in the bacteria compartment but 40–110% more abundant in the attractant compartment than the control over the 48 h period (Figure 3). The greater bacterial migration to higher acetate concentrations in the attractant compartment relative to the control experiment indicated the potential importance of chemotaxis to facilitate bacterial transport to contaminant sources.

The absence of flagella was not sustained over the entire experimental period. Because of favorable growth conditions, bacteria that had their flagella removed likely grew new flagella and subsequently responded chemotactically to acetate after some time. Indeed, it was observed that bacteria that had their flagella removed resumed their motility in 3 h when resuspended in media containing 20 mM acetate and 30 mM urea. As a result, the accumulation difference between two types of bacteria was more apparent at earlier times.

Bacterial Distribution under the Influence of Acetate. Bacterial abundances at 48 h in all three compartments of the filter-chamber are shown in Figure 4. The greatest abundance of bacteria occurred in the sand plug. The bacteria compartment maintained a relatively high abundance primarily due to growth on acetate. The accumulation of bacteria in the attractant compartment was a result of motility, chemotaxis, and growth. It was difficult to distinguish the effect of chemotaxis from the other processes using only the measured bacterial abundances in different compartments. Therefore, we simulated bacterial distributions and compared the results for chemotactic and nonchemotactic bacteria. The bacterial and acetate distributions from the model predictions are superimposed over the averaged bacterial counts in Figure 4.

One difference between the chemotactic test and the control was in the region where the maximum bacterial abundance occurred. The model output in which only growth was considered had the highest abundance in the bacteria compartment, whereas the model output incorporating both chemotactic and growth effects predicted that the highest abundance would occur within the sand plug. This simulation result was in agreement with the experimental data in which the chemotactic bacteria also achieved their greatest abundance in the sand plug. The simulated bacterial abundance in the sand plug was higher than the experimental result, and the difference may be largely due to the sampling procedures employed in the filter-chamber experiments. Because samples were drawn from the bacteria and attractant

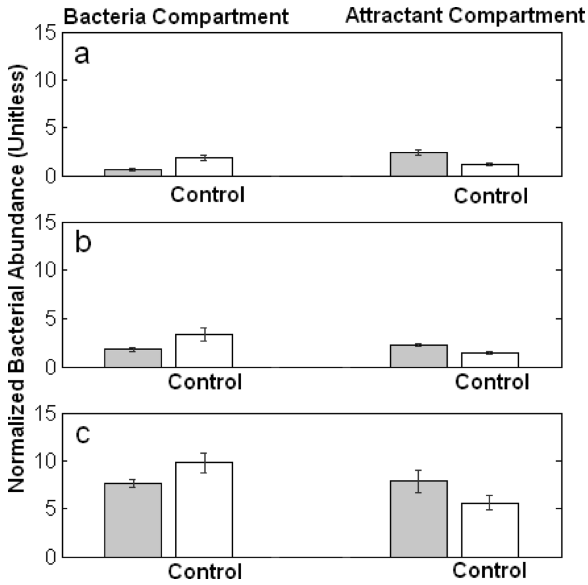

FIGURE 3. Experimental data for chemotactic *P. putida* F1 and nonchemotactic control (obtained by mechanically shearing off the flagella) in the bacteria compartment and the attractant compartment at (a) 13 h, (b) 22 h, and (c) 48 h with an initial acetate concentration of 20 mM. Bacterial abundances are normalized to the initial bacterial abundances in the bacteria compartment. Differences between accumulation of the chemotactic and nonchemotactic bacteria in each compartment were statistically significant ($p = 0.05$). Error bars represent the standard deviation for the bacterial counting processes.

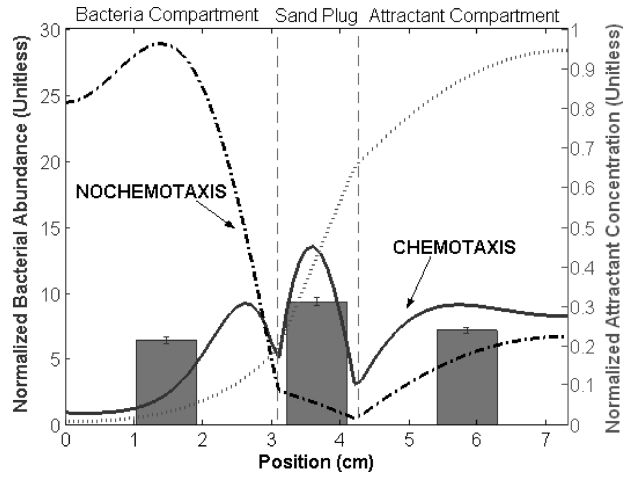

FIGURE 4. *P. putida* F1 abundance distribution (normalized to the initial abundance in bacteria compartment) at 48 h under the influence of 20 mM acetate initially in the attractant compartment. Three replicates were measured for the distribution. The average abundances were $(3.2 \pm 0.3) \times 10^7$ cells/mL in the bacteria compartment, $(4.5 \pm 0.3) \times 10^7$ cells/mL in the sand plug, and $(3.3 \pm 0.2) \times 10^7$ cells/mL in the attractant compartment. The abundance in the sand plug was statistically different from the others ($p = 0.05$). Normalized bacterial abundances predicted by the model are plotted along the one-dimensional filter-chamber length: the first 3.1 cm represents the bacteria compartment, the next 1.2 cm represents the sand plug, and the last 3.1 cm represents the attractant compartment. The bold line is the simulated bacterial profile with chemotaxis at 48 h, which has an average value of 1.9×10^7 cells/mL in the bacteria compartment, 5.5×10^7 cells/mL in the sand plug, and 3.8×10^7 cells/mL in the attractant compartment. The dashed line represents bacteria with the same growth characteristics but no chemotactic response with an average value of 1.1×10^8 cells/mL in the bacteria compartment, 8.0×10^6 cells/mL in the sand plug, and 2.3×10^7 cells/mL in the attractant compartment. Normalized attractant concentrations at 48 h also are plotted as dashed lines for both cases, which appear to be superimposed because the differences are negligible.

compartments before sampling the sand, bacteria may have been drawn out from the sand plug toward both compartments during the extraction process, which may have yielded a lower bacterial abundance measurement in the sand plug and a higher concentration in the bacteria compartment. The lower bacterial population in the attractant compartment may be due to the overestimation of growth without consideration of oxygen supply limitations at 48 h.

The simulated bacterial abundance among the three compartments depended upon as to whether chemotaxis was or was not invoked. In the test (chemotaxis) system, more bacteria migrated up the attractant gradient through the sand plug, resulting in a lower abundance in the bacteria compartment and a higher abundance in the attractant compartment at 48 h. The larger population of chemotactic bacteria in the attractant compartment produced more bacteria by the growth on acetate, which resulted in an even larger bacterial population over time. The location of the peak chemotactic bacterial abundance within the chamber coincided with the attractant concentration at which the bacteria are most sensitive to the attractant. As described in eq 2, the bacterial chemotactic velocity depends on both the attractant concentration and the gradient. Attractant concentrations near the K_c value elicit the strongest chemotactic response, and the bacterial chemotactic velocities are extremely sensitive to the attractant value at this range. Because of the dilution of acetate in the bacteria compartment, the attractant gradient in the sand plug remained steep and relatively constant around the K_c value (*10, 16, 20, 21*). The peak in bacterial abundance in the sand plug at 48 h also indicated that the chemotactic effect was still apparent after considerable bacterial growth. It predicted that chemotaxis yielded bacterial abundance in a favorable region even when coupled with growth over the long period. On the basis of a time-scale analysis, we note that the growth process affects the bacterial distribution over a longer time scale and serves to increase the magnitude of the population, while chemotaxis affects the distribution over a shorter time scale and tends to establish the shape of the distribution.

Field Site Experimental Data. Filter-chamber experiments were conducted in the field with a measured ambient temperature around 10 °C, a measured dissolved oxygen level near 0.1 mg/L, and a natural gradient groundwater flow. The initial acetate concentration was chosen to be 0.1 mM to test a smaller growth effect as compared to the laboratory tests. The average abundances in the bacteria compartments at 15 h in the field chambers were obtained and compared (Figure 2c). With an abundance of $(2.3 \pm 0.6) \times 10^6$ cells/mL, chemotactic bacteria in the presence of acetate influence had a lower population than the controls with no acetate, which was $(4.4 \pm 0.4) \times 10^6$ cells/mL. Although a different strain and a lower initial attractant concentration were used in the field, this result followed the same qualitative trend as the data point at 13 h in Figure 2b (i.e., chemotactic bacteria transported more readily through the sand plug to the acetate source, and fewer bacteria remained in the bacteria compartment).

For both laboratory and field studies, chemotactic bacterial abundances were lower than the no-acetate controls in the bacteria compartments. To support our observations, we applied the mathematical model to the field conditions to verify the trend and to predict the bacterial abundances among compartments within the chambers. In Figure 5, model predictions of bacterial abundances in the attractant and bacteria compartments are plotted as a function of time. Four different situations were simulated: the first one with

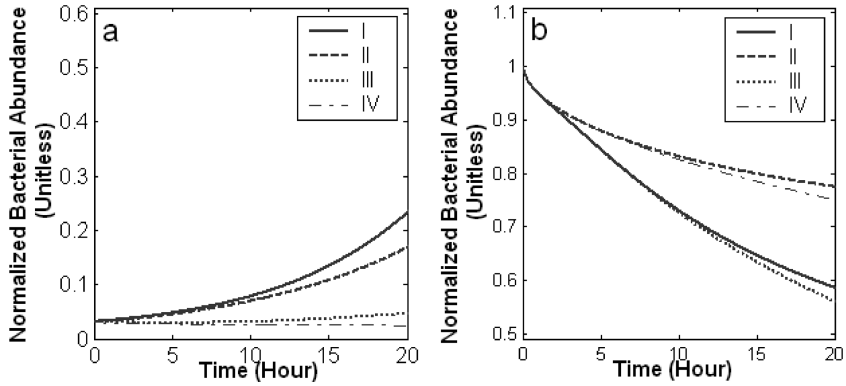

FIGURE 5. Temporal changes in bacterial abundances in both (a) attractant compartment and (b) bacteria compartment estimated by mathematical models for the field site experiments. Four situations were simulated: I, both chemotaxis and growth on acetate; II, growth without chemotaxis; III, chemotaxis without growth; and IV, neither chemotaxis nor growth. An acetate concentration of 0.1 mM was initially loaded in the attractant compartment. We used the same parameter values in the simulations as in Figure 2 except for the chemotactic binding constant (1.56×10^{-5} M) (*20*) to accommodate the low attractant concentration. It was assumed that 97% of initial bacteria was in the bacteria compartment and that 3% of bacteria was in the attractant compartment at $t = 0$ to account for bacteria entering the attractant compartment near the junction of the walls and the sand plug during the initial injection.

chemotactic bacteria, growing in the presence of acetate, therefore undergoing both chemotactic and growth effects; the second one with nonchemotactic bacteria that had the same growth dependence but showed no chemotactic ability to acetate; the third one with only a chemotactic response and no growth; and the fourth one with chemotactic bacteria but no acetate (no chemotaxis or growth). The second and third situations were not feasible in our experiments.

The differences between the model simulations involving chemotactic bacteria and the no-acetate control were consistent with experimental data (i.e., there were more bacteria in the bacteria compartment for the first several hours if there was no acetate available). Because more bacteria were concentrated into the sand zone where the acetate gradient produced the strongest chemotactic response, fewer bacteria were left in the bacteria compartment as compared to the control. Note that the nonchemotactic bacterial abundances with acetate (II in Figure 5b) were always higher than the other three cases, which suggested that growth facilitated the higher bacterial abundances in the bacteria compartment and that chemotaxis needs to be invoked to reduce the bacterial abundances in the bacteria compartment. Because the experimental observations were obtained at a lower temperature (10 °C) in the field (*48*) than the laboratory (25 °C) and because they employed a lower acetate concentration, we expected a lower growth rate; consequently, there were lower bacterial abundances in the field study than the model prediction incorporating laboratory growth parameters.

With experimental results from both laboratory and field studies, we revealed the important role that chemotaxis may play in determining small-scale microbial distributions in the immediate vicinity of a growth-promoting organic contaminant within contaminated granular aquifers. This study suggests that small-scale chemotactic migration is likely to facilitate bioremediation by inducing a greater bacterial abundance near attractant sources. The next important step is to provide direct measurements of contaminant degradation rates that may be enhanced due to increased bacterial abundances. This may be particularly important where contaminants are concentrated in lenses or layers of fine-grained sediments, characterized by a low hydraulic conductivity.

Acknowledgments

The authors gratefully acknowledge John Lisle of the U.S. Geological Survey for construction and assistance with the design of the filter-chambers and David Metge for preparing field test bacteria. Acknowledgment is made to the Donors of the American Chemical Society Petroleum Research Fund (ACS-PRF 38031-AC9) for partial support of this research. This work also was funded by the National Science Foundation (EAR 0408454). Additional support was provided by a fellowship from the NIH Biotechnology Training Program at the University of Virginia. We extend our appreciation to Denis LeBlanc and others of the U.S. Geological Survey for their generous assistance at the field site in Cape Cod, MA. Any use of trade, firm, or product names is for descriptive purposes only and does not imply endorsement by the U.S. Government.

Literature Cited

(1) Ang, E. L.; Zhao, H.; Obbard, J. P. Recent advances in the bioremediation of persistent organic pollutants via biomolecular engineering. *Enzyme Microb. Technol.* **2005**, *37* (5), 487–496.

(2) Pignatello, J. J.; Xing, B. Mechanisms of slow sorption of organic chemicals to natural particles. *Environ. Sci. Technol.* **1996**, *30* (1), 1–11.

(3) Gierczak, R. F. D.; Devlin, J. F.; Rudolph, D. L. Combined use of field and laboratory testing to predict preferred flow paths in a heterogeneous aquifer. *J. Contam. Hydrol.* **2006**, *82* (1–2), 75–98.

(4) Lee, M.; Saunders, J. A.; Wolf, L. W. Effects of geologic heterogeneities on pump-and-treat and in situ bioremediation: A stochastic analysis. *Environ. Eng. Sci.* **2000**, *17* (3), 183–189.

(5) Grimm, A. C.; Harwood, C. S. Chemotaxis of *Pseudomonas* spp. to the polyaromatic hydrocarbon naphthalene. *Appl. Environ. Microbiol.* **1997**, *63* (10), 4111–4115.

(6) Hawkins, A. C.; Harwood, C. S. Chemotaxis of *Ralstonia eutropha* JMP134(pJP4) to the herbicide 2,4-dichlorophenoxyacetate. *Appl. Environ. Microbiol.* **2002**, *68* (2), 968–972.

(7) Marx, R. B.; Aitken, M. D. Bacterial chemotaxis enhances naphthalene degradation in a heterogeneous aqueous system. *Environ. Sci. Technol.* **2000**, *34* (16), 3379–3383.

(8) Parales, R. E.; Haddock, J. D. Biocatalytic degradation of pollutants. *Curr. Opin. Biotechnol.* **2004**, *15* (4), 374–379.

(9) Pandey, G.; Jain, R. K. Bacterial chemotaxis toward environmental pollutants: Role in bioremediation. *Appl. Environ. Microbiol.* **2002**, *68* (12), 5789–5795.

(10) Parales, R. E.; Ditty, J. L.; Harwood, C. S. Toluene-degrading bacteria are chemotactic towards the environmental pollutants benzene, toluene, and trichloroethylene. *Appl. Environ. Microbiol.* **2000**, *66* (9), 4098–4104.

(11) Law, A. M. J.; Aitken, M. D. Bacterial chemotaxis to naphthalene desorbing from a nonaqueous liquid. *Appl. Environ. Microbiol.* **2003**, *69* (10), 5968–5973.

(12) Samanta, S. K.; Singh, O. V.; Jain, R. K. Polycyclic aromatic hydrocarbons: Environmental pollution and bioremediation. *Trends Biotechnol.* **2002**, *20* (6), 243–248.

(13) Harwood, C. S.; Parales, R. E.; Dispensa, M. Chemotaxis of *Pseudomonas putida* toward chlorinated benzoates. *Appl. Environ. Microbiol.* **1990**, *56* (5), 1501–1503.
(14) Parales, R. E.; Harwood, C. S. Bacterial chemotaxis to pollutants and plant-derived aromatic molecules. *Curr. Opin. Microbiol.* **2002**, *5* (3), 266–273.
(15) Witt, M. E.; Dybas, M. J.; Worden, R. M.; Criddle, C. S. Motility-enhanced bioremediation of carbon tetrachloride-contaminated aquifer sediments. *Environ. Sci. Technol.* **1999**, *33* (17), 2958–2964.
(16) Ford, R. M.; Phillips, B. R.; Quinn, J. A.; Douglas, A. L. Measurement of bacterial random motility and chemotaxis coefficients: I. Stopped-flow diffusion chamber assay. *Biotechnol. Bioeng.* **1991**, *37* (7), 647–660.
(17) Lanning, L.; Ford, R. M.; Long, T. Bacterial Chemotaxis Transverse to Axial Flow in a Microfluidic Channel, *Biotechnol. Bioeng.*, **2008**, DOI 10.1002/bit. 21814.
(18) McClaine, J. W.; Ford, R. M. Characterizing the adhesion of motile and nonmotile *Escherichia coli* to a glass surface using a parallel-plate flow chamber. *Biotechnol. Bioeng.* **2002**, *78* (2), 179–189.
(19) Mesibov, R.; Ordal, G. W.; Adler, J. The range of attractant concentrations for bacterial chemotaxis and the threshold and size of response over this range: Weber Law and related phenomena. *J. Gen. Physiol.* **1973**, *62* (2), 203–223.
(20) Kusy, K. Bacterial Migration in Heterogeneous Porous Media. Ph.D Thesis, University of Virginia, Charlottesville, VA, 2006.
(21) Olson, M. S.; Ford, R. M.; Smith, J. A.; Fernandez, E. J. Quantification of bacterial chemotaxis in porous media using magnetic resonance imaging. *Environ. Sci. Technol.* **2004**, *38* (14), 3864–3870.
(22) Pedit, J. A.; Marx, R. B.; Miller, C. T.; Aitken, M. D. Quantitative analysis of experiments on bacterial chemotaxis to naphthalene. *Biotechnol. Bioeng.* **2002**, *78* (6), 626–634.
(23) Roush, C.; Lastoskie, C.; Worden, R. Denitrification and chemotaxis of *Pseudomonas stutzeri* KC in porous media. *J. Environ. Sci. Health, Part A: Toxic/Hazard. Subst. Environ. Eng.* **2006**, *41*, 967–983.
(24) Sherwood, J. L.; Sung, J. C.; Ford, R. M.; Fernandez, E. J.; Maneval, J. E.; Smith, J. A. Analysis of bacterial random motility in a porous medium using magnetic resonance imaging and immunomagnetic labeling. *Environ. Sci. Technol.* **2003**, *37* (4), 781–785.
(25) Atlas, R. M.; Philp, J. *Bioremediation: Applied Microbial Solutions for Real-World Environmental Cleanup*; American Society for Microbiology Press: Washington, DC, 2005.
(26) Langwaldt, J. H.; Puhakka, J. A. On-site biological remediation of contaminated groundwater: A review. *Environ. Pollut.* **2000**, *107* (2), 187–197.
(27) Talley, J. W. *Bioremediation of Relcalcitrant Compounds*; Taylor and Francis Group, LLC: Oxford, 2006.
(28) Pieper, A. P.; Ryan, J. N.; Harvey, R. W.; Amy, G. L.; Illangasekare, T. H.; Metge, D. W. Transport and recovery of bacteriophage PRD1 in a sand and gravel aquifer: Effect of sewage-derived organic matter. *Environ. Sci. Technol.* **1997**, *31* (4), 1163–1170.
(29) Ryan, J. N.; Elimelech, M.; Ard, R. A.; Harvey, R. W.; Johnson, P. R. Bacteriophage PRD1 and silica colloid transport and recovery in an iron oxide-coated sand aquifer. *Environ. Sci. Technol.* **1999**, *33* (1), 63–73.
(30) Adler, J.; Dahl, M. M. A method for measuring the motility of bacteria and for comparing random and non-random motility. *J. Gen. Microbiol.* **1967**, *46*, 161–173.
(31) Kalmokoff, M. L.; Jarrell, K. F.; Koval, S. F. Isolation of flagella from the archaebacterium *Methanococcus voltae* by phase separation with Triton X-114. *J. Bacteriol.* **1988**, *170* (4), 1752–1758.
(32) Kinner, N. E.; Harvey, R. W.; Blakeslee, K.; Novarino, G.; Meeker, L. D. Size-selective predation on groundwater bacteria by nanoflagellates in an organic-contaminated aquifer. *Appl. Environ. Microbiol.* **1998**, *64* (2), 618–625.
(33) Mills, A. L.; Herman, J. S.; Hornberger, G. M.; Dejesus, T. H. Effect of solution ionic-strength and iron coatings on mineral grains on the sorption of bacterial-cells to quartz sand. *Appl. Environ. Microbiol.* **1994**, *60* (9), 3300–3306.
(34) Dong, H. L.; Onstott, T. C.; Ko, C. H.; Hollingsworth, A. D.; Brown, D. G.; Mailloux, B. J. Theoretical prediction of collision efficiency between adhesion-deficient bacteria and sediment grain surface. *Colloids Surf., B* **2002**, *24* (3–4), 229–245.
(35) Fieschko, J.; Humphrey, A. E. Acetate inhibition of *Pseudomonas putida*. *Biotechnol. Bioeng.* **1985**, *27* (9), 1362–1366.
(36) Hobbie, J. E.; Daley, R. J.; Jasper, S. Use of nucleopore filters for counting bacteria by fluorescence microscopy. *Appl. Environ. Microbiol.* **1977**, *33* (5), 1225–1228.
(37) LeBlanc, D. R. *Sewage Plume in a Sand and Gravel Aquifer, Cape Cod, Massachusetts*; Water-Supply Paper 2218; U.S. Geological Survey: Reston, VA, 1984; p 28.
(38) Hess, K. M.; Wolf, S. H.; Celia, M. A. Large-scale natural gradient tracer test in sand and gravel, Cape Cod, Massachusetts. 3. Hydraulic conductivity variability and calculated macrodispersivities. *Water Resour. Res.* **1992**, *28* (8), 2011–2027.
(39) Elliott, L. F.; Gilmour, C. M. Growth of *Pseudomonas stutzeri* with nitrate and oxygen as terminal electron acceptors. *Soil Biol. Biochem.* **1971**, *3* (4), 331–335.
(40) Harvey, R. W.; Garabedian, S. P. Use of colloid filtration theory in modeling movement of bacteria through a contaminated sandy aquifer. *Environ. Sci. Technol.* **1991**, *25* (1), 178–185.
(41) Ford, R. M.; Harvey, R. W. Role of chemotaxis in the transport of bacteria through saturated porous media. *Adv. Water Resour.* **2007**, *30* (6–7), 1608–1617.
(42) Ginn, T. R.; Wood, B. D.; Nelson, K. E.; Scheibe, T. D.; Murphy, E. M.; Clement, T. P. Processes in microbial transport in the natural subsurface. *Adv. Water Resour.* **2002**, *25* (8–12), 1017–1042.
(43) Keller, E. F.; Segel, L. A. Traveling bands of chemotactic bacteria: A theoretical analysis. *J. Theor. Biol.* **1971**, *30* (2), 235–248.
(44) Chen, K. C.; Ford, R. M. Pertubation expansion of Alt's cell balance equations reduces to Segel's one-dimensional equations for shallow chemoattractant gradients. *SIAM J. Appl. Math.* **1998**, *59*, 35–57.
(45) Cussler, E. L. *Diffusion: Mass Transfer in Fluid Systems*, 2nd ed.; Cambridge University Press: New York, 1997.
(46) Huang, W. E.; Oswald, S. E.; Lerner, D. N.; Smith, C. C.; Zheng, C. Dissolved oxygen imaging in a porous medium to investigate biodegradation in a plume with limited electron acceptor supply. *Environ. Sci. Technol.* **2003**, *37* (9), 1905–1911.
(47) Barton, J. W.; Ford, R. M. Determination of effective transport coefficients for bacterial migration in sand columns. *Appl. Environ. Microbiol.* **1995**, *61* (9), 3329–3335.
(48) Harvey, R. W.; Mayberry, N.; Kinner, N. E.; Metge, D. W.; Novarino, F. Effect of growth conditions and staining procedure upon the subsurface transport and attachment behaviors of a groundwater protist. *Appl. Environ. Microbiol.* **2002**, *68* (4), 1872–1881.

ES702392H